A microfluidic step-emulsification device with nozzles arrayed on a slit

Chunqi Zheng[1], Shuzo Masui[2], Yusuke Kanno[2], Takasi Nisisako[2,#]

1 Department of Mechanical Engineering, School of Engineering, Tokyo Institute of Technology, Japan
2 Institute of Innovative Research, Tokyo Institute of Technology, R2-9, 4259 Nagatsuta-cho, Midori-ku, Yokohama, Kanagawa, 226-8503 Japan
Corresponding Author / Email: nisisako.t.aa@m.titech.ac.jp, TEL: +81-45-924-5092, FAX: +81-45-924-5466

KEYWORDS: Step emulsification, Vertical slit, Droplet accumulation, Monodisperse

In conventional step-emulsification devices, accumulation and coalescence of droplets near the nozzles have been an issue. Here, we propose a new step-emulsification device capable of generating highly monodisperse droplets without their accumulation and coalescence. Our device consists of parallel channels where the dispersed and continuous phases flow towards each other and a vertical slit in the middle of the channels where the two phases meet to generate droplets by the step-emulsification regime. Using a device with 16 nozzles (nozzle end: 110 μm wide and 16 μm deep), we could generate monodisperse oil-in-water droplets with an average diameter of 62 μm and a coefficient-of-variation (CV) value of 2.5% with a maximum productivity of ~784 drops/s. Similarly, a device with 128 nozzles (nozzle end: 120 μm wide and 16 μm deep) could produce monodisperse droplets with a mean diameter of 67 μm and a CV of 2.6% at ~4096 drops/s.

NOMENCLATURE

Q_d = flow rate of dispersed phase
Q_c = flow rate of continuous phase
CV = coefficient of variation

1. Introduction

Microfluidic droplet generation has been widely studied for numerous medical diagnostics and material production applications. Among many methods, step emulsification, which is an interfacial-tension-driven method, is known to be robust because droplet size relies on the nozzle geometry and is insensitive to the flow fluctuations of the two phases. Because of this advantage, the volume throughput in step emulsification can be easily scaled up via parallelization of many nozzles[1]. However, droplet accumulation near the nozzles has been a limitation in conventional devices, affecting subsequent and neighboring droplet generation processes. For example, it prevents the backflow of the continuous phase needed for droplet pinch-off[2]. Also, accumulation of the droplets near the nozzles tends to promote their coalescence, producing polydisperse droplets[3].

We recently reported a simple microfluidic step-emulsification device that can prevent droplet accumulation near the nozzles[4]. This device consists of a polydimethylsiloxane (PDMS) chip having an array of microfluidic channels and a stainless-steel block having vertical slit channels (Fig. 1). The disperse and continuous phases meet at the middle slit where step emulsification occurs to produce monodisperse droplets. Then, the continuous phase stream smoothly carries the droplets away from the nozzles through the vertical slit, preventing their accumulation near the nozzles. Using a device having 16 nozzles, for example, we could produce monodisperse droplets with an average diameter of ~80 μm and a CV below 3%.

This paper reports the results of more detailed investigations on a similar 16-nozzle device, including the effect of flow rates on droplet size and size distribution. Also, we present a new device with 128 nozzles prepared to increase the volume throughput.

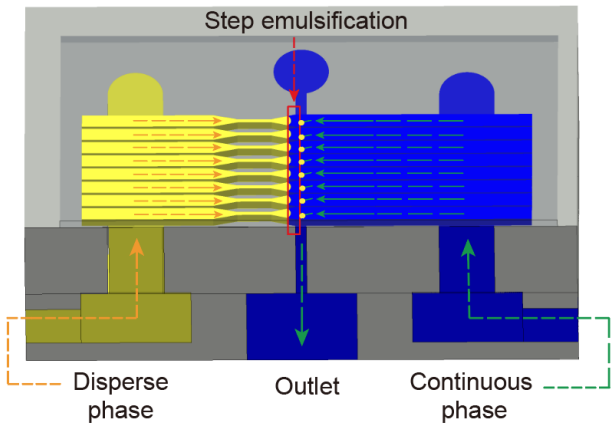

Fig. 1 A schematic illustration of a device with step-emulsification nozzles arrayed on a slit.

2. Experimental

2.1 Device design

We prepared two devices with 16 and 128 nozzles (Table 1). These devices consist of a polydimethylsiloxane (PDMS) chip with an array of parallel microgrooves and stainless-steel parts assembled, as shown in Fig. 2a. Wedge-shaped nozzles of 16-μm depth are located in the middle of the microgrooves on the microfluidic chip (Fig. 2b). The stainless module has two layers (Fig. 2c). The top layer has three vertical slit channels with a pitch of 3 mm; the width of the middle slit is 100 μm, the width of the side slits is 500 μm. The bottom layer has two holes for inlets (diameter, 1 mm) and one middle slit with a width of 1 mm for an outlet.

2.2 Device fabrication

The PDMS chip was fabricated by conventional soft lithography. The layers of stainless steel (SUS304) were made by conventional mechanical machining, including wire electric discharge machining. The PDMS chip was bonded with the top layer by oxygen plasma treatment under 20 W for 90 s, and screws assembled the two stainless-steel layers. The edge of the nozzles on the PDMS chip was precisely aligned with the middle vertical slit. For the generation of oil-in-water (O/W) droplets, the assembled device underwent hydrophilic surface modification via infusion of a reagent solution (SPRA 202, Tokyo Ohka Kogyo, Japan).

2.3 Materials

A 2.0 wt% aqueous solution of polyvinyl alcohol (Mitsubishi Chemical, Japan) was used as the continuous phase. An acrylate monomer, 1,6-hexanediol diacrylate (Kyoeisha, Tokyo, Japan), was used as the disperse phase.

2.4 Equipment

A plastic syringe (volume 5 ml; Terumo, Japan) was set on a syringe pump (Legato 180, KD Scientific, USA) to infuse the disperse phase. A plastic syringe (volume 50 ml; Terumo, Japan) was set on a syringe pump (Legato 200, KD Scientific, USA) to infuse the continuous phase.

The droplet generation process was observed by using an optical microscope (BX51, Olympus, Japan) equipped with a high-speed video camera (Fastcam Mini AX50, Photron, Japan). The droplet sizes and generation rate were analyzed by the free software ImageJ (National Institutes of Health, MD, USA).

3. Results and discussion

3.1 Droplet generation in the 16-nozzle device

When the appropriate flow rates were set for the disperse and continuous phases, we could observe typical droplet formation in step emulsification at all 16 nozzles. Figure 3 shows the droplet generation when Q_d and Q_c were set at 0.35 and 20.0 mL/h, respectively. Under this flow condition, droplets of uniform size were reproducibly generated at all 16 nozzles along the middle slit. From the video, the droplet generation rate in 16 nozzles was 784 drops/s, suggesting that the average droplet generation per nozzle was 49 drops/s.

Table 1 The length of slit and parameters of nozzles.

The number of nozzles (N)	The length of slit (L)	The height of nozzle (H)	The width of nozzle (W)
16	5.5 mm	16 μm	110 μm
128	28.0 mm	16 μm	120 μm

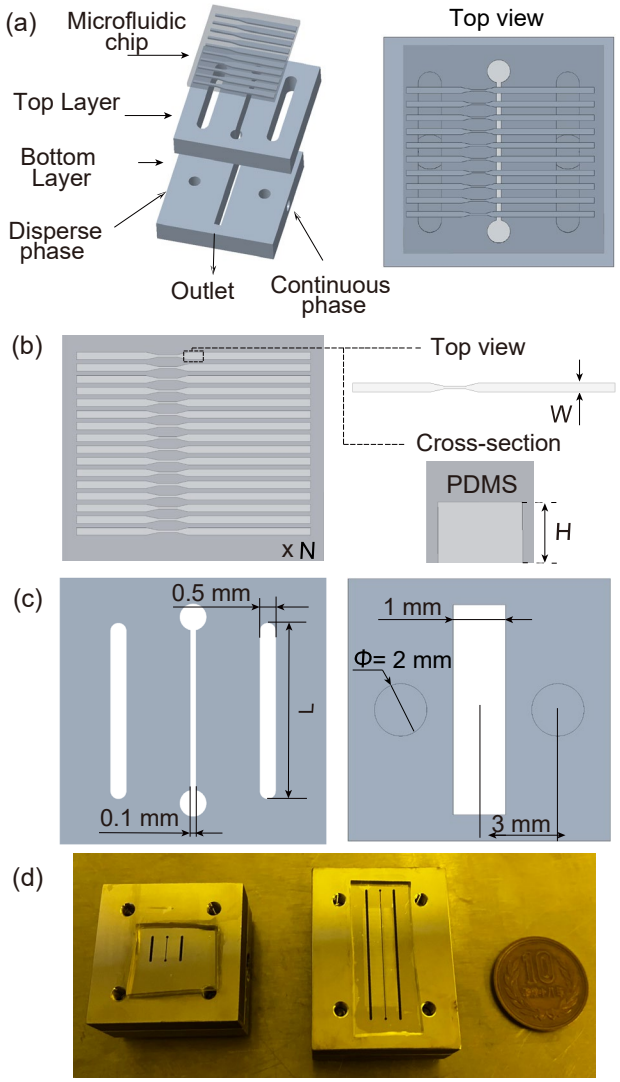

Fig. 2 A microfluidic step-emulsification device with nozzles on a slit. (a) Schematic illustration of the device assembly. (b) Microfluidic chip with paralleled channels and views of the nozzle. (c) Top view of stainless-steel layers. (d) A photograph of the 16-nozzle (left) and 128-nozzle (right) devices.

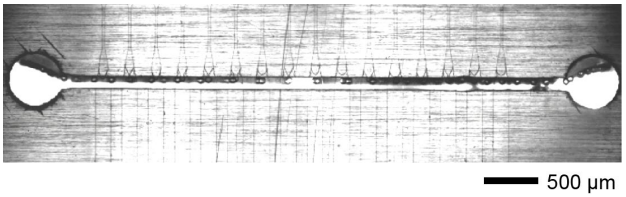

Fig. 3 A top-view photomicrograph showing the generation of droplets in dripping mode in the 16-nozzle device. Flow rates were at Q_c = 0.35 mL/h and Q_d = 20.0 mL/h.

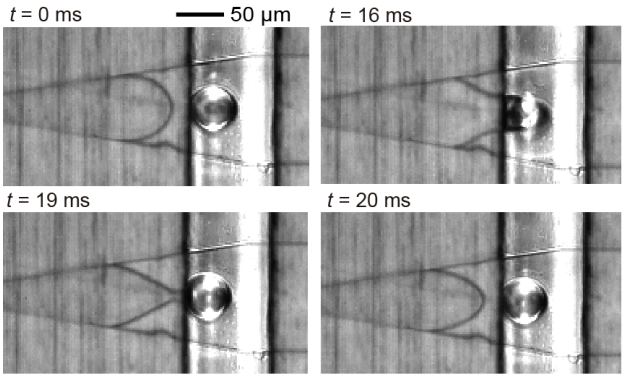

Fig. 4 Time-lapse photomicrographs showing the necking and break-off of a droplet at a nozzle.

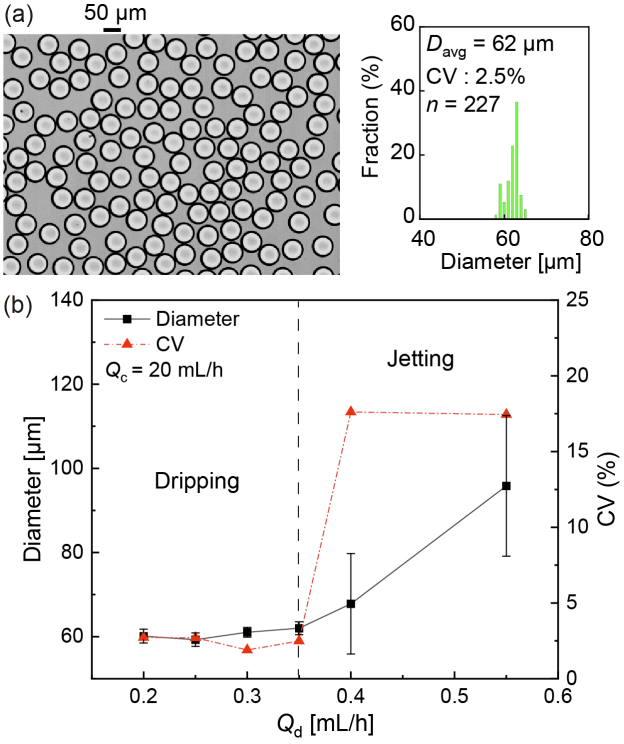

Fig. 5 Droplets produced by the 16-nozzle device. (a) A photomicrograph and size distribution of the droplets produced when Q_d and Q_c were 0.35 and 20.0 mL/h, respectively. (b) The diameter and CV of droplets as a function of Q_d for Q_c = 20.0 mL/h.

Figure 4 is a series of highspeed photomicrographs showing the pinch-off process in one nozzle. In the beginning stage (t = 0 ms), the disperse phase moved forward inside the nozzle, forming a tongue-shaped oil-water interface. After the tongue-shaped interface reached the slit, a droplet formed in the slit and then grew rapidly (t = 16 ms). Along with the droplet growth, necking was observed in the nozzle (t = 19 ms). Then, the droplet was finally broken off, and the disperse phase retracted to start the formation of next droplet (t = 20 ms). Thus, we confirmed the typical transformation of the oil-water interface in step emulsification[1,2].

The produced droplets were collected and observed on a slide glass by optical microscopy. When the flow rates Q_d and Q_c were 0.35 and 20.0 mL/h, respectively, the collected droplets were monodisperse, with an average diameter of 62 μm and a CV of 2.5% (n =225, Fig. 5b). This suggests that no coalescence occured among the droplets after their formation.

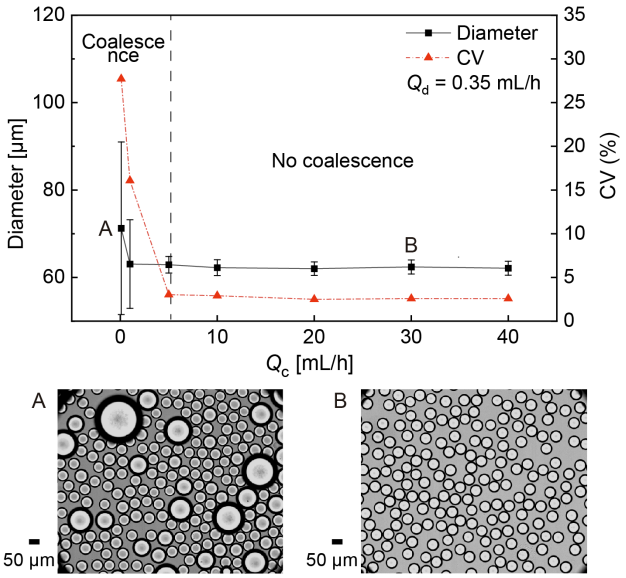

Fig. 6 The effect of Q_c on the diameter and CV of droplets produced in the 16-nozzle device at Q_d = 0.35 mL/h. Inset A is polydisperse droplets after accumulation-induced coalescence at lower Q_c. Inset B is monodisperse droplets collected at higher Q_c.

Next, we varied Q_d under a constant Q_c (=20.0 mL/h) to investigate how Q_d affects the droplet size and size distribution (Fig. 5b). When Q_d was in the range from 0.2 to 0.35 mL/h, the collected droplets were monodisperse with CV values below 3%, and their average diameters did not change significantly within the range of 60 ± 2 μm. This result suggests that all the nozzles produced droplets under this flow-rate range in the dripping regime. However, we found a significant increase in CV values and average diameters when Q_d was set above 0.35 mL/h. For example, when Q_d was set at 0.4 mL/h, some nozzles started jetting to produce bigger droplets with diameters over 90 μm, and the collected droplets had an average size of 68 μm with a CV of 17.6% (n = 229). When Q_d increased to 0.55 mL/h, we observed more nozzles operating in jetting regime, and the collected droplets had an average diameter of 96 μm with a CV of 17.5% (n =137). Thus, we judged that the maximum Q_d under which monodisperse droplets could be obtained in this device was 0.35 mL/h.

Furthermore, we varied Q_c under a constant Q_d (= 0.35 mL/h) to verify the effect of Q_c on the droplet size and size distribution (Fig. 6). When Q_c was set in the range from 5.0 to 40.0 mL/h, monodisperse droplets were produced with similar average diameters (62 ± 1 μm) and CV values below 3%. This similarity in average sizes proves that the droplets were produced by step emulsification, not by viscous shearing from the continuous phase stream. However, the collected droplets became polydisperse when Q_c was set below 5.0 mL/h. For example, when Q_c was set at 0.1 mL/h, the average diameter and CV of the collected droplets were 71 μm and 27.7% (n = 272), respectively. The increase in the average size and CV was presumably due to the accumulation-induced coalescence of densely packed droplets near the nozzles. Thus, we confirmed that Q_c needed to be high enough to avoid the accumulation of droplets near the nozzles for the off-chip collection of monodisperse droplets.

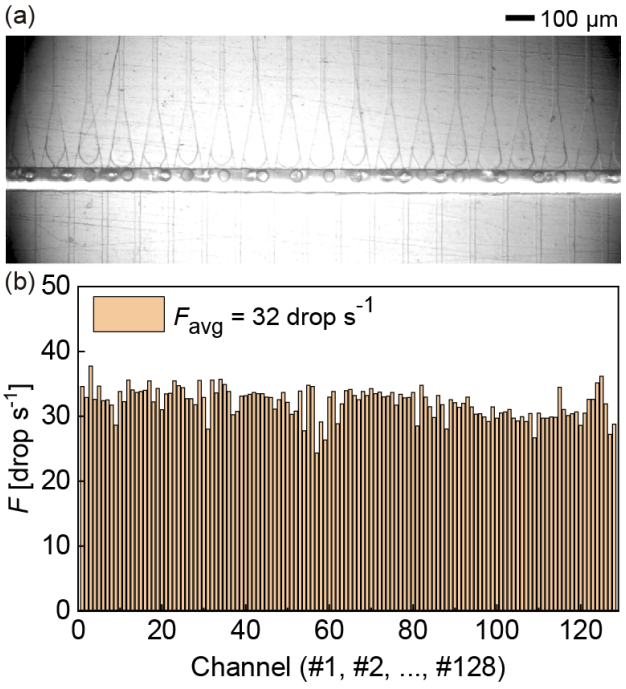

Fig. 7 Generation of droplets in the 128-nozzle device. (a) A photomicrograph of the nozzles producing droplets. (b) Distribution of droplet generation rates at each nozzle when Q_d and Q_c are 2.4 and 20.0 mL/h, respectively.

3.2 Droplet generation in the 128-nozzle device

For the scaled-up production of monodisperse droplets, we prepared and tested the 128-nozzle device. For example, droplets of uniform size were generated in the dripping mode at the 128 nozzles when Q_d and Q_c were set at 2.4 and 20.0 mL/h, respectively (Fig. 7a). From the video, the droplet generation rate in total was measured to be ~4096 drops/s, meaning that the generation rate per nozzle was ~32 drops/s (Fig. 7b). The produced droplets had an average diameter of 67 μm with a CV of 2.6% (n = 188, Fig. 8a), suggesting that no coalescence occurred after their formation. Although the generation rate per channel had a certain variation among the nozzles (CV: 7.1%), the produced droplets were measured to be monodisperse. This result supports that the droplets were generated under the principle of step emulsification, in which droplet size is insensitive to flow fluctuations.

As in the 16-nozzle device, accumulation-induced coalescence yielded polydisperse droplets when Q_c was sufficiently low in the 128-nozzle device (Fig. 8b). When Q_c was set at 1.0 mL/h, the average droplet size was 78 μm with a CV of 20% (n = 149). In contrast, when we varied Q_c in the range from 20 to 80 mL/h with Q_d fixed at 2.4 mL/h, the droplets were kept monodisperse with similar average diameters of 67 ± 1 μm and CV values less than 3%.

4. Conclusions

Microfluidic step-emulsification devices with 16 or 128 nozzles arrayed on a vertical slit were proposed and tested to generate monodisperse droplets. The continuous phase stream effectively carried the droplets away from the nozzles, thereby avoiding

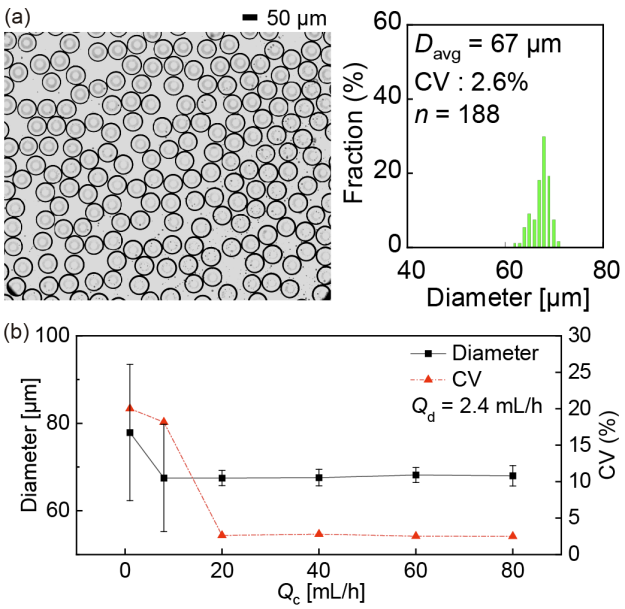

Fig. 8 Droplets produced by the 128-nozzle device. (a) A photomicrograph and size distribution of the off-chip droplets produced at Q_d = 2.4 mL/h and Q_c = 20 mL/h. (b) The effect of Q_c on the diameter and CV of the droplets produced at Q_d = 2.4 mL/h.

accumulation and coalescence among the droplets. The effects of dispersed and continuous phase flow rates on droplet size and size distributions were studied. The maximum productivity of the 16-nozzle device was 784 drops/s with an average droplet size of 62 μm and a CV of 2.5%. The 128-nozzle device could generate monodisperse droplets with a CV under 3% at a generation rate of 4096 drops/s.

ACKNOWLEDGEMENT

This work was supported by JSPS KAKENHI Grant Number 20H02512.

REFERENCES

1. Liu, Z., Duan, C., Jiang, S., Zhu, C., Ma, Y. and Fu, T., "Microfluidic step emulsification techniques based on spontaneous transformation mechanism: a review," J. Ind. Eng. Chem., Vol. 92, pp. 18–40, 2020.
2. Shi, Z., Lai, X., Sun, C., Zhang, X., Zhang, L., Pu, Z., Wang, R., Yu, H. and Li, D., "Step emulsification in microfluidic droplet generation: mechanisms and structures," Chem. Commun., Vol. 56, No. 64, pp. 9056–9066, 2020.
3. Ji, G., Kanno, Y. and Nisisako, T., "Microfluidic coupling of step emulsification and deterministic lateral displacement for producing satellite-free droplets and particles," Micromachines, Vol. 14, No. 3, 622, 2023.
4. Zheng, C., Ji, G., Masui, X., Kanno, Y. and Nisisako, T., "Microfluidic step emulsification via parallel nozzles crossing a slit," 2023 JSPE Spring Meeting, pp. 597–598, 2023.